

# Optical Properties of Synthetic Cannabinoids with Negative Indexes

Yao Shen<sup>1,\*</sup> and Yu-Zhu Chen<sup>2</sup>

<sup>1</sup>School of Forensic Science, People's Public Security University of China, Beijing 100038, PR China

<sup>2</sup>Department of Physics, Tianjin University, Tianjin 300350, PR China

\*shenyaophysics@hotmail.com

## ABSTRACT

Some kinds of psychoactive drugs have the structures which are called split-ring resonators (SRRs). SRRs might result in negative permittivity and permeability simultaneously in electromagnetic field. Simultaneous negative indexes can lead to the famous phenomenon of negative refraction. This optical property makes it possible to distinguish synthetic cannabinoids from other abusive psychoactive drugs in the UV-vis region. This optical method is non-damaged and superior in forensic science. In this paper, we use tight-binding model calculating the permittivity and permeability of the main ingredients of synthetic cannabinoids. At the same time, we give two more results of zolpidem and caffeine. Further we discuss the negative refraction of the category of zepam qualitatively.

In 1968, Veselago originally introduced the concept of negative index material (NIM) which exhibit unusual optical property.<sup>1</sup> For this kind of material, the permittivity and permeability can be negative simultaneously in electromagnetic field, which might bring about the phenomenon of negative refraction. Pendry *et al.*<sup>2-6</sup> developed Veselago's theory, their research pointed out that the configuration of split-ring resonators (SRRs)<sup>3</sup> which had non-trivial symmetry breaking<sup>7</sup> is an effective way to realize negative refraction. Negative refraction has become more and more popular these decades, new researches and applications come to practice. For instance, the perfect lenses which are made by NIM can focus all Fourier components of image, both their propagating and evanescent waves are amplified, the quality of image and the detection sensitivity are improved.<sup>8-12</sup> After the theoretical derivation, Shelby *et al.*<sup>13</sup> gave the experimental realization two years later. According to Veselago's theory, molecules with SRRs configurations such as extended metal atom chains (EMACs), have led a fresh direction of physical and chemical research.<sup>14-37</sup> Recently many fabulous works in different fields come forth, such as invisible cloaking,<sup>38-43</sup> liquid crystal magnetic control,<sup>44</sup> anapole moment,<sup>45</sup> detection of latent fingerprints,<sup>46-48</sup> etc. Inspired by these ideas, negative refraction plays more and more important role in forensic science field since it is a non-damaged optical method to test materials. More importantly, a small categories of molecules could show negative response to electromagnetic fields.<sup>49</sup> Utilizing this property, these categories of molecules can be distinguished from others. This is significant to differentiate psychoactive drugs in forensic science. As a matter of fact, according to the theoretical derivation and calculation, we point out that the main ingredients of synthetic cannabinoids, the category of zepam, zolpidem and caffeine show various degree of negative refraction while other psychoactive drugs can not. We discuss the result of synthetic cannabinoids, zolpidem and caffeine quantitatively and the category of zepam qualitatively.

This paper is organized as following: In section II, we previously derive the permittivity and permeability of the main ingredients of synthetic cannabinoids, zolpidem and caffeine theoretically. Subsequently in section III, the numerical results of permittivity and permeability are discussed. Finally, the main results are concluded and future work is predicted in section IV.

## Theoretical Derivation

### Hückel Model and Tight-binding Method

According to Pendry's research, molecules which have the broken ring configurations can realize special optical property which is called negative refraction. We find that the main ingredients of synthetic cannabinoids such as JWH-018 (K2), JWH-073 (K2), AKB48 (K3) and AM2201 (K3) have the architecture of SRRs, therefore, their permittivity and permeability can be negative simultaneously in electromagnetic field. Moreover, two more compounds zolpidem and caffeine can also reveal negative refraction. In this section, we mainly discuss three kinds of model of synthetic cannabinoids, zolpidem and caffeine.

Figure 1(a) demonstrates the configuration of AKB48 (apinaca) molecule, and Figure 1 (b) is the structure called AM2201. The systematic name of AKB48 is N-(1-adamantyl)-1-pentyl-1H-indazole-3-carboxamide, and that of AM2201 is 1-(5-fluoropentyl)-3-(1-naphthoyl)indole. They are the main ingredients of K3 (synthetic cannabinoids).

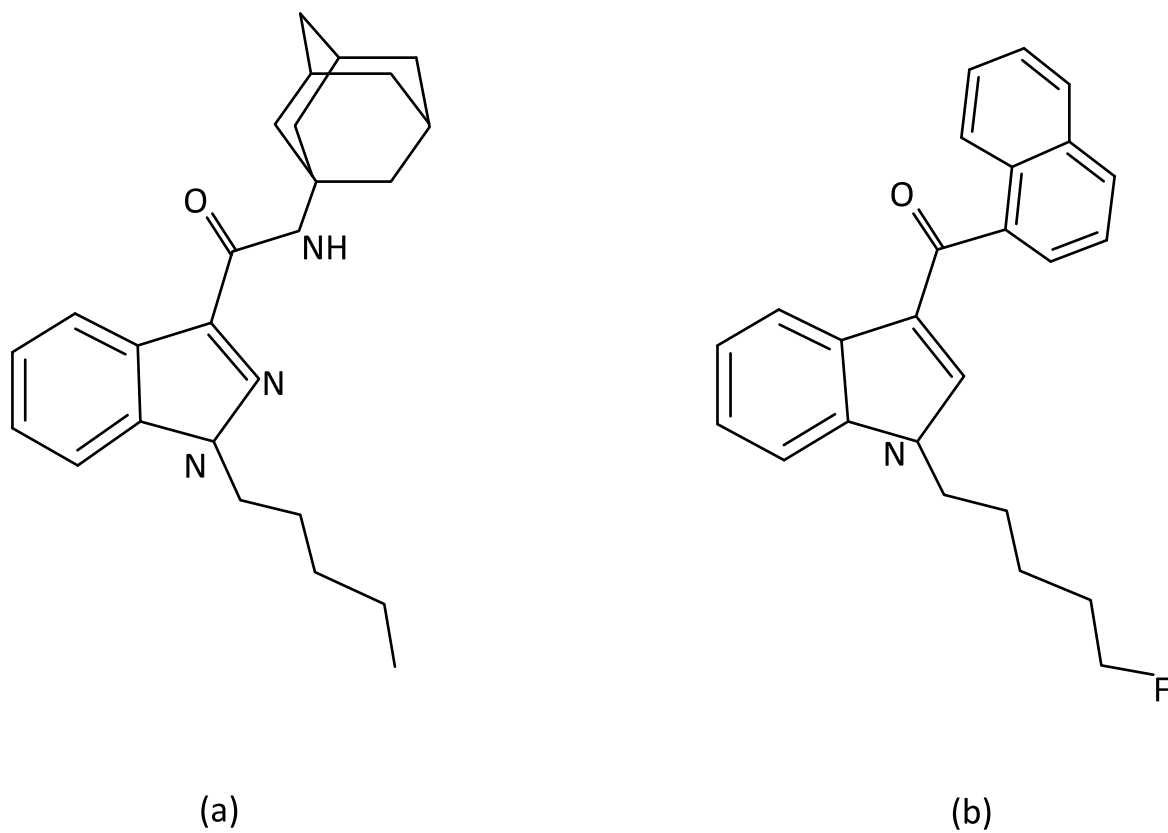


**Figure 1.** (a)The molecule of AKB48 (Apinaca,  $C_{23}H_{31}N_3O$ ). AKB48 is N-(1-adamantyl)-1-pentyl-1H-indazole-3-carboxamide. (b)The molecule of AM2201 ( $C_{24}H_{22}FN$ ). AM2201 is 1-(5-fluoropentyl)-3-(1-naphthoyl)indole.

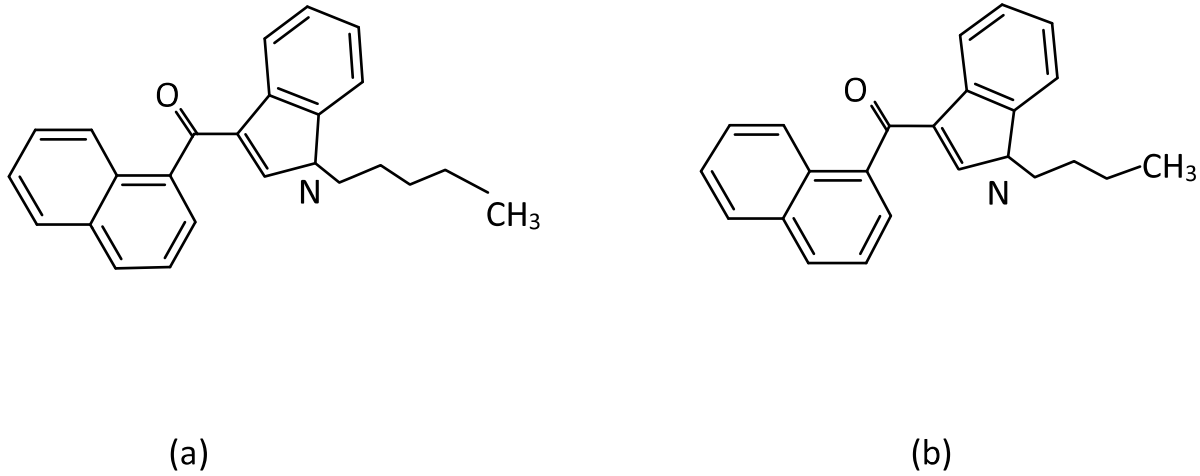


**Figure 2.** (a)The molecule of JWH-018. JWH-018 is 1-pentyl-3-(1-naphthoyl)indole ( $C_{24}H_{23}NO$ ). (b)The molecule of JWH-073. JWH-073 is naphthalen-1-yl-(1-butylindol-3-yl)methanone ( $C_{23}H_{21}NO$ ).

Figure 2(a) shows the structure of JWH-018 molecule, Figure 2(b) gives us JWH-073 molecule. JWH-018 is 1-pentyl-3-(1-naphthoyl)indole and JWH-073 is naphthalen-1-yl-(1-butylindol-3-yl)methanone. They are the main ingredients of K2 (synthetic cannabinoids).

Both K2 and K3 are synthetic cannabinoids. The central parts of them are the broken ring of pentagons. These broken pentagons contribute to the negative refraction mostly, because all these phenomena come from the  $\pi$  electrons of conjugate ring of these molecules which are called single-nitrogen-substituted heterocyclic annulenes.<sup>50</sup> For AKB48, two carbon atoms of the pentagon are substituted with two nitrogen atoms, while for AM2201, JWH-018 and JWH-073, only one carbon atom of the pentagon is replaced by one nitrogen atom. The simplified model are given in following Figure 3. The left figure is the simplified model of AKB48 and the ringt one is the model of AM2201, JWH-018 and JWH-073. All the atoms of the pentagon are in the same plane and be marked as Figure 3.

The simplified model of AKB48 has two nitrogen atoms which are located at site 4 and 5. The other model has only one nitrogen atom which is placed at site 5. These two models are called 1H-pyrazole and pyrrole respectively.

There are two other cases in psychoactive drugs which also have broken conjugate ring. The simplified model of zolpidem and caffeine is given in Figure 4. There are also two nitrogen atoms instead of two carbon atoms, but their positions are quite different from 1H-pyrazole. Therefore, these dissimilar simplified models show different degree of negative refraction.

The Hückel Hamiltonian of these five  $\pi$  electrons conjugate systems are described as<sup>51</sup>

$$\mathcal{H} = \sum_{j=1}^5 \alpha_j |j\rangle \langle j| + \sum_{j=1}^5 \beta_{j,j+1} (|j\rangle \langle j+1| + |j+1\rangle \langle j|), \quad (1)$$

where  $j$  denotes the site lable,  $\alpha$  is site energy and  $\beta$  is the resonant integral. When  $j = 5$ , we have  $j + 1 = 1$ , because of the ring configuration. We choose  $\alpha_C = -6.7eV$ ,  $\alpha_N = -7.9eV$ .<sup>53</sup> The resonant integral given by Harrison expression<sup>54,55</sup>

$$\beta_{ij} = -0.63 \frac{\hbar^2}{m d_{ij}^2} \quad (2)$$

where  $m$  is the mass of electrons and  $d_{ij}$  expresses the bond length. All data come from NIST.<sup>56</sup>

- 1H-pyrazole (AKB48)

$$\mathcal{H} = \sum_{j=1}^3 \alpha_C |j\rangle \langle j| + \alpha_N (|4\rangle \langle 4| + |5\rangle \langle 5|) + \sum_{j=1}^5 \beta_{j,j+1} (|j\rangle \langle j+1| + |j+1\rangle \langle j|), \quad (3)$$

where  $\beta_{1,2} = -2.545eV$ ,  $\beta_{2,3} = -2.393eV$ ,  $\beta_{3,4} = -2.708eV$ ,  $\beta_{4,5} = -2.632eV$ ,  $\beta_{5,1} = -2.598eV$ .

- pyrrole (AM2201, JWH-018 and JWH-073)

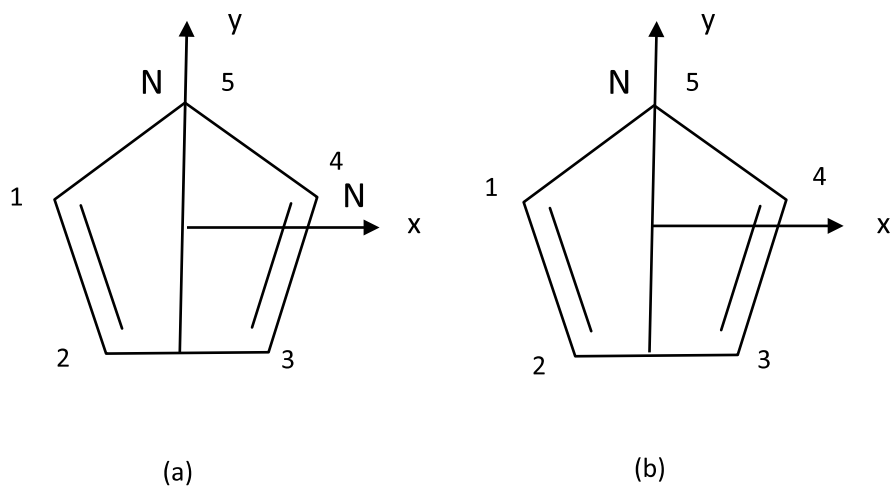


**Figure 3.** The Simplified models of synthetic cannabinoids. (a) The model of AKB48 is 1H-pyrazole ( $C_3H_4N_2$ ) on the left. (b) The models of AM2201, JWH-018 and JWH-073 are all pyrrole ( $C_4H_5N$ ) on the right. The origin is set at the center of the pentagons.

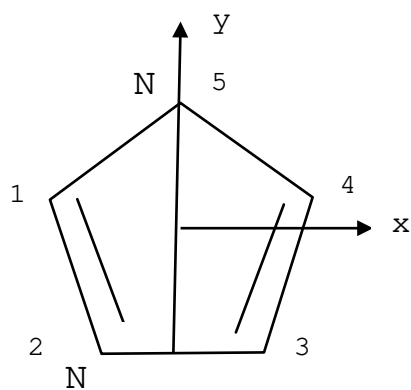


**Figure 4.** The Simplified models of zolpidem and caffeine are both 1H-imidazole ( $C_3H_4N_2$ ). 1H-imidazole is different from 1H-pyrazole, although they have the same molecular formula. The nitrogen atoms are located at different sites.

$$\mathcal{H} = \sum_{j=1}^4 \alpha_C |j\rangle \langle j| + \alpha_N |5\rangle \langle 5| + \sum_{j=1}^5 \beta_{j,j+1} (|j\rangle \langle j+1| + |j+1\rangle \langle j|), \quad (4)$$

where  $\beta_{1,2} = -2.516eV$ ,  $\beta_{2,3} = -2.393eV$ ,  $\beta_{3,4} = -2.516eV$ ,  $\beta_{4,5} = -2.560eV$ ,  $\beta_{5,1} = -2.560eV$ .

- 1H-imidazole (zolpidem and caffeine)

$$\mathcal{H} = \sum_{j=1,3,4} \alpha_C |j\rangle \langle j| + \alpha_N (|2\rangle \langle 2| + |5\rangle \langle 5|) + \sum_{j=1}^5 \beta_{j,j+1} (|j\rangle \langle j+1| + |j+1\rangle \langle j|), \quad (5)$$

where  $\beta_{1,2} = -2.783eV$ ,  $\beta_{2,3} = -2.516eV$ ,  $\beta_{3,4} = -2.582eV$ ,  $\beta_{4,5} = -2.534eV$ ,  $\beta_{5,1} = -2.582eV$ .

By diagonalizing the Hückel Hamiltonian, we calculate the energy levels of these models as Figure 5.

$$\mathcal{H} = \sum_{k=1}^5 \varepsilon_k |\psi_k\rangle \langle \psi_k|, \quad (6)$$

where

$$|\psi_k\rangle = \sum_{j=1}^5 C_{kj} |j\rangle \quad (7)$$

$\varepsilon_k$  is the eigen value and  $|\psi_k\rangle$  is the eigen states. Not losing the generality, we shift all energy levels by  $\alpha_C$  for simplicity.

- 1H-pyrazole (AKB48)

$\varepsilon_1 = -5.762eV$ ,  $\varepsilon_2 = -2.109eV$ ,  $\varepsilon_3 = -1.966eV$ ,  $\varepsilon_4 = 3.465eV$ ,  $\varepsilon_5 = 3.972eV$ .

- pyrrole (AM2201, JWH-018 and JWH-073)

$\varepsilon_1 = -5.330eV$ ,  $\varepsilon_2 = -1.972eV$ ,  $\varepsilon_3 = -1.590eV$ ,  $\varepsilon_4 = 3.708eV$ ,  $\varepsilon_5 = 3.983eV$ .

- 1H-imidazole (zolpidem and caffeine)

$\varepsilon_1 = -5.734eV$ ,  $\varepsilon_2 = -2.472eV$ ,  $\varepsilon_3 = -1.743eV$ ,  $\varepsilon_4 = 3.694eV$ ,  $\varepsilon_5 = 3.855eV$ .

All energy levels are nondegenerated. We have five non-interacting  $\pi$  electrons fill in five energy levels. On the basis of Pauli exclusion principle, the energy of ground state is  $E_0 = 2\varepsilon_1 + 2\varepsilon_2 + \varepsilon_3$ . And the second-quantization form of the ground state can be expressed as

$$|\Psi_0\rangle = a_{1\uparrow}^\dagger a_{1\downarrow}^\dagger a_{2\uparrow}^\dagger a_{2\downarrow}^\dagger a_{3\uparrow}^\dagger |0\rangle, \quad (8)$$

where  $|0\rangle$  is vacuum state and  $a_{p\sigma}^\dagger$  is the creation operator of the orbital  $p$  with spin  $\sigma$  ( $\sigma = \uparrow, \downarrow$ ).

We only consider the single-excitation with no flip of electronic spin. All these three kinds of systems have fourteen single-excitation states.

The single-excitation states of the system which denote the single electron excitation from  $p$  to  $q$  can be assumed as

$$|\Psi_n\rangle = |\Psi_{qp}^\sigma\rangle = a_{q\sigma}^\dagger a_{p\sigma} |\Psi_0\rangle, \quad (9)$$

where  $p = 1, 2, 3$ ,  $q = 3, 4, 5$  and  $\sigma = \uparrow, \downarrow$ . The corresponding energies are

$$E_n = E_0 + \varepsilon_q - \varepsilon_p. \quad (10)$$

The ground state and single-excitation states span a subspace. In this subspace, the Hamiltonian reads

$$\mathcal{H} = \sum_{n=0}^{14} E_n |\Psi_n\rangle \langle \Psi_n|. \quad (11)$$

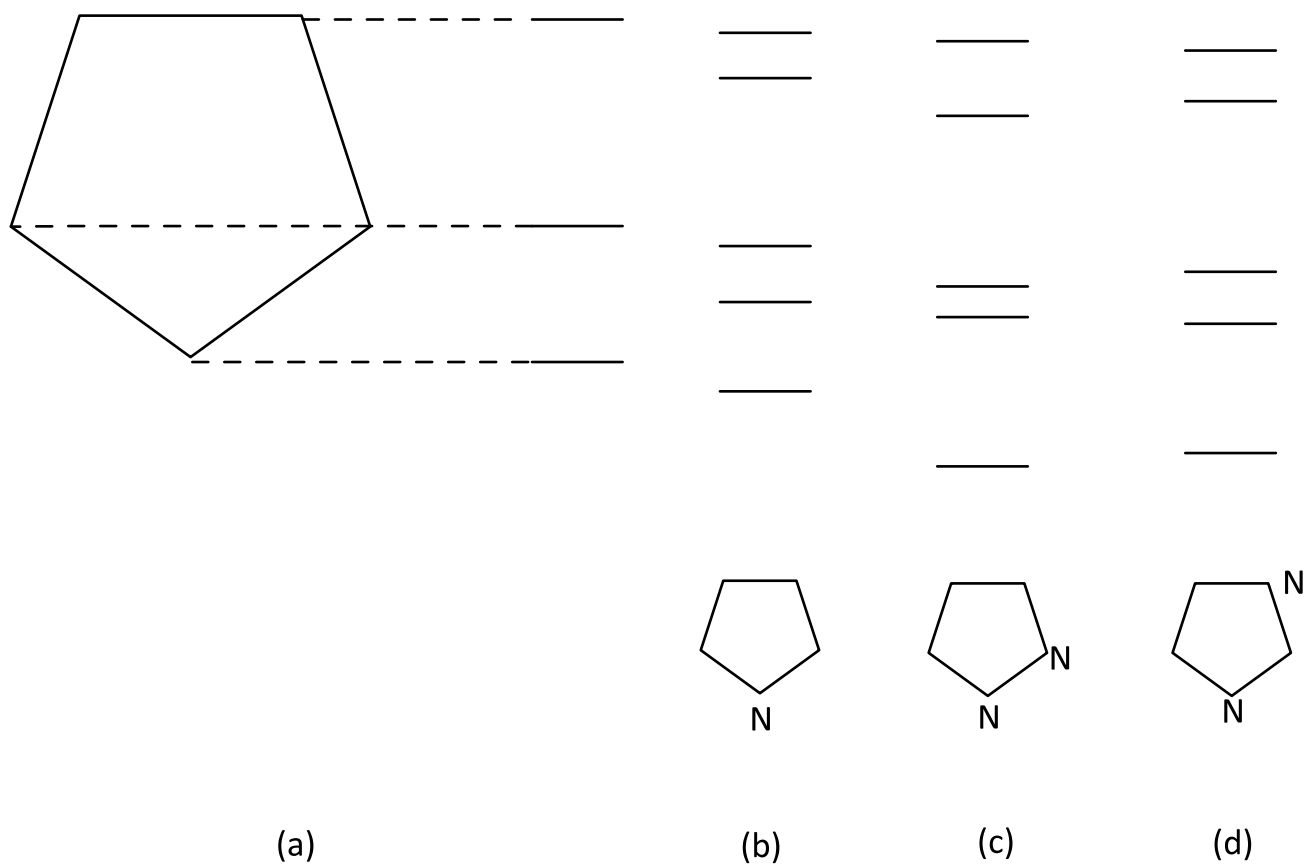


**Figure 5.** (a) The energy levels of 1,3-cyclopentadiene ( $C_5H_6$ ). (b) The energy levels of pyrrole ( $C_4H_5N$ ). (c) The energy levels of 1H-pyrazole ( $C_3H_4N_2$ ). (d) The energy levels of 1H-imidazole ( $C_3H_4N_2$ ).

## Perturbation Theory in Electromagnetic Field

When the molecules are placed in a time-dependent electromagnetic field, the total Hamiltonian with the dipole approximation can be written as

$$H = H_0 - \vec{\mu} \cdot \vec{E}_0 \cos(\vec{k} \cdot \vec{r} - \omega t) - \vec{m} \cdot \vec{B}_0 \cos(\vec{k} \cdot \vec{r} - \omega t), \quad (12)$$

where  $\vec{k}$  is the wave vector,  $\vec{\mu}$  is the electric dipole moment,  $\vec{m}$  is the magnetic dipole moments and  $H_0 = \mathcal{H}$  as defined above is the Hamiltonian without electromagnetic field. Because the spatial scale of electromagnetic wave length is much longer than that of the molecules, we assume that the spatial part of the electromagnetic field can be neglected.

$$H \simeq H_0 - \vec{\mu} \cdot \vec{E}_0 \cos(\omega t) - \vec{m} \cdot \vec{B}_0 \cos(\omega t). \quad (13)$$

By a unitary transformation, the Hamiltonian can be simplified into a time independent one in Schrodinger picture. In this picture, the state and operator are  $|\Psi'\rangle = U^\dagger |\Psi\rangle$ , and  $A' = U^\dagger A U$ . The Hamiltonian of the system can be rewritten as

$$\begin{aligned} H' &= U^\dagger H U - iU^\dagger \dot{U} \\ &\simeq \sum_{n=1}^{14} E_n |\Psi_n\rangle \langle \Psi_n| + (E_0 + \omega) |\Psi_0\rangle \langle \Psi_0| + H'', \end{aligned} \quad (14)$$

where

$$U = \exp(i\omega |\Psi_0\rangle \langle \Psi_0| t), \quad (15)$$

$$\begin{aligned} H'' &= -\frac{1}{2} \sum_{n=1}^{14} [ (\vec{\mu}_{n0} \cdot \vec{E}_0 |\Psi_n\rangle \langle \Psi_0| + \vec{\mu}_{0n} \cdot \vec{E}_0 |\Psi_0\rangle \langle \Psi_n|) \\ &\quad + (\vec{m}_{n0} \cdot \vec{B}_0 |\Psi_n\rangle \langle \Psi_0| + \vec{m}_{0n} \cdot \vec{B}_0 |\Psi_0\rangle \langle \Psi_n|) ], \end{aligned} \quad (16)$$

$$\vec{\mu}_{ns} = \langle \Psi_n | \vec{\mu} | \Psi_s \rangle, \quad (17)$$

$$\vec{m}_{ns} = \langle \Psi_n | \vec{m} | \Psi_s \rangle. \quad (18)$$

Moreover, according to the perturbation theory, the molecular ground state in Schrodinger picture becomes

$$|\Psi'_0\rangle = U^\dagger |\Psi_0\rangle = |\Psi_0\rangle + \sum_{n=1}^{14} \frac{\langle \Psi_n | H'' | \Psi_0 \rangle}{E_0 + \omega - E_n} |\Psi_n\rangle, \quad (19)$$

### Derivation of Permittivity

The electric dipole moment in Schrodinger picture is

$$\vec{\mu}' = U^\dagger \vec{\mu} U = \sum_{n=1}^{14} (\vec{\mu}_{n0} e^{i\omega t} |\Psi_n\rangle \langle \Psi_0| + \vec{\mu}_{0n} e^{-i\omega t} |\Psi_0\rangle \langle \Psi_n|). \quad (20)$$

And its expectation value in ground state reads

$$\langle \Psi'_0 | \vec{\mu}' | \Psi'_0 \rangle = -\text{Re} \sum_{n=1}^{14} \frac{\vec{\mu}_{n0} \cdot \vec{E}_0}{E_0 + \omega - E_n} \vec{\mu}_{0n} e^{-i\omega t}. \quad (21)$$

So the electric moment for  $N$  identical molecules can be expressed as

$$\vec{P} = - \sum_{s=1}^N \sum_{n=1}^{14} \frac{[\vec{\mu}_{n0}(s) \cdot \vec{E}_0] \vec{\mu}_{0n}(s)}{E_0 + \omega - E_n}. \quad (22)$$

According to the theory of the electric displacement field in the electromagnetic field, we have

$$\vec{D} = \epsilon \vec{E}_0 = \epsilon_0 \epsilon_r \vec{E}_0 = \epsilon_0 \vec{E}_0 + \frac{\vec{P}}{V}, \quad (23)$$

where  $V$  is the volume and  $\vec{P}$  is the electric moment. Thus, the relative permittivity can be written as

$$\epsilon_{ij}^r \equiv \delta_{ij} - \sum_{s=1}^N \sum_{n=1}^{14} \frac{\vec{\mu}_{0n}(s) \cdot \hat{e}_i \vec{\mu}_{n0}(s) \cdot \hat{e}_j}{\epsilon_0 V (E_0 + \omega - E_n)}, \text{ for } i, j = x, y, z, \quad (24)$$

where  $\hat{e}_i$  is the unit vector of the lab coordinate system.

The origin of the simplified model is set at the center of the pentagons (see Figure 3, 4). As we known, the electric dipole moment reads

$$\vec{\mu} = - \sum_{j=1}^5 e \vec{r}_j, \quad (25)$$

where  $-e$  is the electric charge and  $\vec{r}_j$  is the location vector. Therefore, in the eigen states of molecules, the electric dipole moment operators are

$$\vec{\mu}_{mn} = \langle \Psi_m | \vec{\mu} | \Psi_n \rangle = -e \sum_{j=1}^5 \langle \Psi_m | \vec{r}_j | \Psi_n \rangle = -e \sum_{j=1}^5 \langle \psi_f | \vec{r}_j | \psi_g \rangle = -e \sum_{j=1}^5 C_{fj}^* C_{gj} \vec{r}_j, \quad (26)$$

where  $\psi_g$  denotes single electron orbital.

#### Derivation of Permeability

As we known, the magnetic dipole moment can be written as

$$\vec{m} = \frac{-e}{2m_e} \vec{L}, \quad (27)$$

where  $\vec{L}$  is the angular momentum of the system. According to the the Heisenberg equations, we have  $L_x = L_y = 0$ ,

$$\begin{aligned} L_z &= xp^y - yp^x \\ &= \frac{1}{2} (xp^y + p^y x - yp^x - p^x y) \\ &= im_e (x\mathcal{H}y - y\mathcal{H}x). \end{aligned} \quad (28)$$

In this case, the magnetic dipole moment can be rewritten as

$$\begin{aligned} \vec{m} &= \frac{-e}{2m_e} L_z \hat{e}_z \\ &= \frac{-ie}{2} (x\mathcal{H}y - y\mathcal{H}x) \hat{e}_z \\ &= \frac{-ie}{2} \sum_{p,q} \sum_n E_n (x_{pn} y_{nq} - y_{pn} x_{nq}) |\Psi_p\rangle \langle \Psi_q| \hat{e}_z, \end{aligned} \quad (29)$$

where  $x_{pn} = \langle \Psi_p | x | \Psi_n \rangle$ ,  $y_{nq} = \langle \Psi_n | y | \Psi_q \rangle$ .

Similarly in Schrodinger picture, the expectation value of magnetic dipole moment in ground state is

$$\langle \Psi_0 | \vec{m}' | \Psi_0 \rangle = -\text{Re} \sum_{n=1}^{14} \frac{\vec{m}_{n0} \cdot \vec{B}_0}{E_0 + \omega - E_n} \vec{m}_{0n} e^{-i\omega t}. \quad (30)$$

So the magnetic dipole moment for  $N$  identical molecules can be expressed as

$$\vec{M} = - \sum_{s=1}^N \sum_{n=1}^{27} \frac{\mu_0 \vec{m}_{n0}(s) \cdot \vec{B}_0}{E_0 + \omega - E_n} \vec{m}_{0n}(s). \quad (31)$$

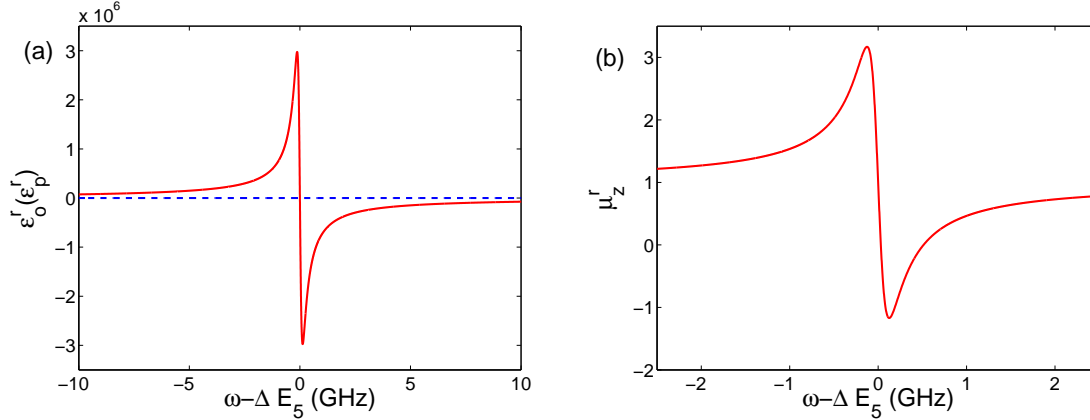


**Figure 6.** The numerical simulation of (a) permittivity and (b) permeability of pyrrole ( $C_4H_5N$ , including AM2201, JWH-018 and JWH-073) vs the frequency  $\omega$  of the electromagnetic field. The axis  $o$  is one main axis in the  $xy$  plane while the axis  $p$  is another main axis in this plane. (a) The permittivity  $\epsilon_o^r$  (red solid line) is negative around the resonance frequency, while  $\epsilon_p^r$  (blue dashed line) is always certain constant. (b) The permeability along  $z$  direction  $\mu_z^r$  can be negative around the resonance frequency simultaneously.

The magnetic induction in a volume  $V$  can be expressed as

$$\vec{B} = \mu \vec{H} = \mu_0 \mu_r \vec{H} = \mu_0 \vec{H} + \mu_0 \frac{\vec{M}}{V}, \quad (32)$$

where  $\vec{H}$  is magnetic field intensity.

The relative permeability of system can be expressed as

$$\mu_{ij}^r \equiv \delta_{ij} - \mu_0 \sum_{s=1}^N \sum_{n=1}^{14} \frac{\vec{m}_{0n}(s) \cdot \hat{e}_i \vec{m}_{n0}(s) \cdot \hat{e}_j}{V(E_0 + \omega - E_n)}, \text{ for } i, j = x, y, z. \quad (33)$$

### Analysis of Analytical Results

For negative refraction, the permittivity and permeability of the system should be negative simultaneously. On the basis of the analytical results given above (24) and (33), the second parts of these two equations should be greater than unity, even far exceed. In this case, we reckon that the denominators are much smaller than the numerator apparently which means  $E_0 + \omega - E_n \approx 0$  and  $\omega \approx E_n - E_0$ .  $E_0$  is the ground state energy of initial state. When the molecules are placed in electromagnetic field, the electromagnetic field gives them a driving frequency  $\omega$  which made them transit to the final state with energy  $E_n$ . Here only single electron excitation is taken into account. The negative refraction, or in another word, simultaneous negative permittivity and permeability occurs while the driving frequency of electromagnetic field  $\omega$  approximately equal to the difference of the energy  $E_n - E_0$ .

### Numerical Simulation of Permittivity and Permeability

The analytical results of section suggest that in certain frequency regime the molecules of certain psychoactive drugs can demonstrate negative refraction in the UV-vis region. These psychoactive drugs mainly include synthetic cannabinoids, zolpidem and caffeine. In this section, we show the numerical results and analyses to corroborate it. These molecules of psychoactive drugs can be simplified into three kinds of two dimensional models (see Figure 3 and Figure 4). Figure 6 gives the numerical simulation of permittivity and permeability of pyrrole ( $C_4H_5N$ ) which is the simplified model of AM2201, JWH-018 and JWH-073. Figure 7 is the result of AKB48 (1H-pyrazole ( $C_3H_4N_2$ )). Figure 8 shows the permittivity and permeability of zolpidem and caffeine (1H-imidazole ( $C_3H_4N_2$ )). All these permittivities  $\epsilon_r$  are in the  $xy$  plane, while permeabilities  $\mu_r$  are in  $z$  direction of the systems. We suppose that the life time of the excited-state is  $\tau = 10\text{ns}$ .<sup>52</sup> For pyrrole ( $C_4H_5N$ ) the main contribution comes from the transition to the fifth excited state, e.g. a electron transits from  $\epsilon_3$  to  $\epsilon_5$  with no flip. And the third transition makes the major contribution to negative indexes of 1H-pyrazole ( $C_3H_4N_2$ ). While for zolpidem and caffeine,

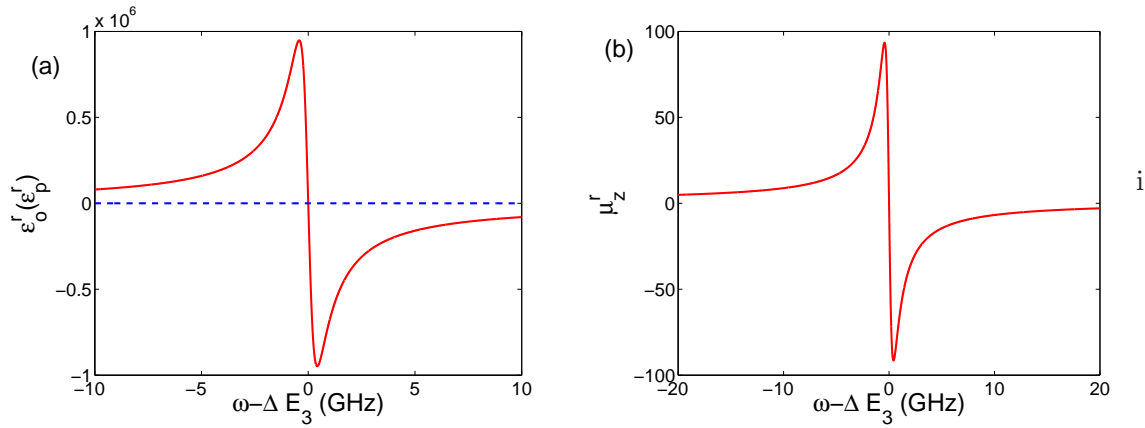


**Figure 7.** The numerical simulation of (a) permittivity and (b) permeability of AKB48 (1H-pyrazole ( $C_3H_4N_2$ )) vs the frequency  $\omega$  of the electromagnetic field. The axis  $o$  is one main axis in the  $xy$  plane while the axis  $p$  is another main axis in this plane. (a) The permittivity  $\epsilon_o^r$  (red solid line) can be negative around the resonance frequency. (b) The permeability along  $z$  direction  $\mu_z^r$  can also be negative around the resonance frequency simultaneously.

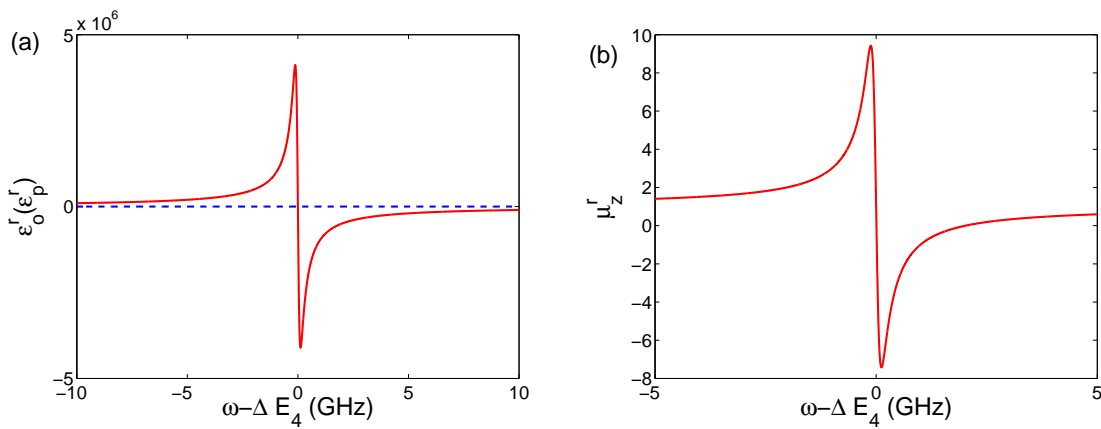


**Figure 8.** The numerical simulation of (a) permittivity and (b) permeability of zolpidem and caffeine (1H-imidazole ( $C_3H_4N_2$ )) vs the frequency  $\omega$  of the electromagnetic field. The axis  $o$  is one main axis in the  $xy$  plane while the axis  $p$  is another main axis in this plane. (a) The negative permittivity  $\epsilon_o^r$  (red solid line) and constant  $\epsilon_p^r$  (blue dashed line) are shown. (b) The negative permeability along  $z$  direction  $\mu_z^r$  is also given.

which hails from the transition to the forth excited state. All these molecules display negative permittivity and permeability simultaneously, thereby bring negative refraction consequently. For negative magnetic response, the permeability of AKB48 is much more obvious than that of the others (about 10 times). While the result of permittivity is reversed (about 3 to 5 times in  $10^6$ ). The phenomenon of negative refraction of AM2201, JWH-018, JWH-073, zolpidem and caffeine are of significant to AKB48. To achieve negative permittivity and permeability simultaneously, the pickwidths of AKB48 in the figure are wider than others. In other words, the pickwidths reveals that AKB48 is much easier to realize negative refraction at the present stage.

## Conclusion and Discussion

In this paper we put forward a new method to identify certain kinds of psychoactive drugs which have the structures called split-ring resonators. This configuration might induce negative permittivity and permeability simultaneously, consequently negative refraction in the UV-vis region. When light with certain frequency transmit through the transparent media which has psychoactive drugs with negative indexes on it, the refracted light goes on the opposite side comparing with the ordinary case. Namely in common case, when the incident light transmit onto the surface of media, the refracted light lies on the contrary side of normal. But for negative refraction material, the refracted light and incident light lie on the same side of normal. This phenomenon made us capable of distinguishing certain families of psychoactive drugs from others. The optical method has its advantage which is non-damaged and would not cumber the detection of DNA in forensic science. Here we use Hückel model to deal with the systems. As a result, we conclude that the main ingredients of synthetic cannabinoids, zolpidem and caffeine can show various degree of negative refraction, thereby can be distinguished from others. In psychoactive artificial cannabinoid families e.g. AM-xxx, HU-xxx, JWH-xxx, CP xx, other small quantity of ingredients e.g. AM-694, JWH-250 can also give the result of negative refraction but they are un conspicuous. It is a remarkable fact that the category of zepam which has a broken ring of heptagon could also give negative refraction in all psychoactive drugs. But the category of zepam is not a prevalent abused drug as synthetic cannabinoids and others, therefore we only give analytic derivation and numerical simulation of three simplified models.

## Acknowledgement

The research was supported by NSF of China under Grant No. 11575125. We thank for the useful discussion of Pro. Wu-Sheng Dai from Department of Physics, Tianjin University.

## References

1. Veselago, V. G. The electrodynamics of substances with simultaneously negative values of  $\epsilon$  and  $\mu$ . *Sov. Phys. Uspekhi* **10**, 509-514 (1968).
2. Pendry, J. B. Negative refraction makes a perfect lens. *Phys. Rev. Lett.* **85**, 3966-3969 (2000).
3. Pendry, J. B., Holden, A. J., Robbins, D. J. & Stewart, W. J. Magnetism from conductors and enhanced nonlinear phenomena. *IEEE Trans. Microwave Theory Tech.* **47**, 2075-2084 (1999).
4. Pendry, J. B., Holden, A. J., Stewart, W. J. & Youngs, I. Extremely low frequency plasmons in metallic mesostructures. *Phys. Rev. Lett.* **76**, 4773-4776 (1996).
5. Pendry, J. B., Holden, A. J., Robbins, D. J. & Stewart, W. J. Low frequency plasmons in thin-wire structures. *J. Phys. Condens. Matter* **10**, 4785-4809 (1998).
6. Luo, Y., Zhao, R. K., Fernandez-Dominguez, A. I., Stefan, A. M. & John, P. B. Harvesting light with transformation optics. *Sci. Chin. Inf. Sci.* **56**, 120401 (2013).
7. Fang, Y. N., Shen, Y., Ai, Q. & Sun, C. P. Negative refraction induced by Möbius topology. *Preprint arXiv:1501.05729*.
8. Pendry, J. B., Holden, A. J., Robbins, D. J., Stewart, W. J. Magnetism from conductors and enhanced nonlinear phenomena. *IEEE Trans. Microwave Theory Tech.* **47**, 2075, (1999).
9. Cubukcu, E., Zhang, S., Park, Y.-S., Bartal, G. & Zhang, X. Split ring resonator sensors for infrared detection of single molecular monolayers. *Appl. Phys. Lett.* **95**, 043113 (2009).
10. Clark, A. W., Glidle, A., Cumming, D. R. S. & Cooper, J. M. Plasmonic split-ring resonators as dichroic nanophotonic {DNA} biosensors. *J. Am. Chem. Soc.* **131**, 176150-17619 (2009).
11. Pryce, I. M., Kelaita, Y. A., Aydin, K., Briggs, R. M. & Atwater, H. A. Compliant metamaterials for resonantly enhanced infrared absorption spectroscopy and refractive index sensing. *ACS Nano* **5**, 8167-8174 (2011).

12. Ma, C. B., Aguinaldo, R. & Liu, Z. W. Advances in the hyperlens. *Chin. Sci. Bull.* **55**, 2618-2624 (2010).
13. Shelby, R. A., Smith, D. R. & Schultz, S. Experimental verification of a negative index of refraction. *Science* **292**, 77-79 (2001).
14. Ropp, C. *et al.* Positioning and immobilization of individual quantum dots with nanoscale precision. *Nano Lett.* **10**, 4673-4679 (2010).
15. Cao, J. J. *et al.* Dielectric optical-controllable magnifying lens by nonlinear negative refraction. *Sci. Rep.* **5**, 11892 (2015).
16. Bi, K. *et al.* Negative and near zero refraction metamaterials based on permanent magnetic ferrites. *Sci. Rep.* **4**, 4139 (2014).
17. Philippe, F. D., Murray, T. W., Prada, C. Focusing on plates: controlling guided waves using negative refraction. *Sci. Rep.* **5**, 11112 (2015).
18. Smith, D. R., Pendry, J. B. & Wiltshire, M. C. K. Metamaterials and negative refractive index. *Science* **305**, 788-792 (2004).
19. Decker, M., Linden, S. & Wegener, M. Coupling effects in low-symmetry planar split-ring resonator arrays. *Opt. Lett.* **34**, 1579-1581 (2009).
20. Pryce, I. M., Aydin, K., Kelaita, Y. A., Briggs, R. M. & Atwater, H. A. Highly strained compliant optical metamaterials with large frequency tunability. *Nano Lett.* **10**, 4222-4227 (2010).
21. Chen, W. T. *et al.* Optical magnetic response of upright plasmonic molecules in 3D metamaterial. *SPIE News-room* **2011**.
22. Liu, N., Liu, H., Zhu, S. & Giessen, H. Stereometamaterials. *Nat. Photonics* **3**, 157-162 (2009).
23. Fleming, G. R. & Wolynes, P. G. Chemical dynamics in solution. *Phys. Today* **43**, 36-43 (1990).
24. Szabo, A. & Ostlund, N. S. *Modern quantum chemistry: Introduction to advanced electronic structure theory* (Dover, New York, 1996).
25. Greenwood, H. H. *Computing methods in quantum organic chemistry* (Wiley-Interscience, Germany, 1972).
26. Pantazis, D. A. & McGrady, J. E. A three-state model for the polymorphism in linear tricobalt compounds. *J. Am. Chem. Soc.* **128**, 4128-4135 (2006).
27. Pyrka, G. J., El-Mekki, M. & Pinkerton, A. A. Structure of the linear trinuclear copper complex, dichlorotetrakis-(di-2-pyridylamido)tricopper. *J. Chem. Soc., Chem. Commun.* 84-85 (1991).
28. Peng, S.-M. *et al.* One-dimensional metal string complexes. *J. Magn. Magn. Mater.* **209**, 80-83 (2000).
29. Tsai, T.-W., Huang, Q.-R., Peng, S.-M. & Jin, B.-Y. Smallest electrical wire based on extended metal-atom chains. *J. Phys. Chem. C* **114**, 3641-3644 (2010).
30. Chae, D.-H. *et al.* Vibrational excitations in single trimetal-molecule transistors. *Nano Lett.* **6**, 165-168 (2006).
31. Chen, I.-W. P. *et al.* Conductance and stochastic switching of ligand-supported linear chains of metal atoms. *Angew. Chem. Int. Edit.* **45**, 5814-5818 (2006).
32. Chen, C. C. *et al.* Fabrication of three dimensional split ring resonators by stress-driven assembly method. *Opt. Express* **20**, 9415-9420 (2012).
33. Ishikawa, A. & Tanaka, T. J. Two-photon fabrication of three-dimensional metallic nanostructures for plasmonic metamaterials. *Laser Micro Nanoeng.* **7**, 11-15 (2012).
34. Shen, Y. & Jin, B.-Y. Correspondence between Gentile oscillators and N-annulenes. *J. Phys. Chem. A* **117**, 12540-12545 (2013).
35. Shen, Y., Dai, W. S. & Xie, M. Intermediate-statistics quantum bracket, coherent state, oscillator, and representation of angular momentum [SU(2)] algebra. *Phys. Rev. A* **75**, 042111 (2007).
36. Shen, Y., Ai, Q. & Long, G. L. The relation between properties of Gentile statistics and fractional statistics of anyon. *Phys. A* **389**, 1565-1570 (2010).
37. Zhang, S. & Zhang, Y. Broadband unidirectional acoustic transmission based on piecewise linear acoustic metamaterials. *Chin. Sci. Bull.* **59**, 3239-3245 (2014).
38. Pendry, J. B., Schurig, D. & Smith, D. R. Controlling electromagnetic fields. *Science* **312**, 1780-1782 (2006).

39. Schurig, D. *et al.* Metamaterial electromagnetic cloak at microwave frequencies. *Science* **314**, 977-980 (2006).
40. Huang, Y. & Gao, L. Equivalent permittivity and permeability and multiple Fano resonances for nonlocal metallic nanowires. *J. Phys. Chem. C* **117**, 19203-19211 (2013).
41. Droulias, S. & Yannopapas, V. Broad-band giant circular dichroism in metamaterials of twisted chains of metallic nanoparticles. *J. Phys. Chem. C* **117**, 1130-1135 (2013).
42. Xue, H. J., Wu, R. L. & Yu, Y. Abnormal absorption and energy flow of electromagnetic wave in ultrathin metal films. *J. Phys. Chem. C* **118**, 18257-18262 (2014).
43. Yannopapas, V. & Psarobas, I. E. Ordered arrays of metal nanostrings as broadband super absorbers. *J. Phys. Chem. C* **116**, 15599-15603 (2012).
44. Kaelberer, T., Fedotov, V. A., Papasimakis, N., Tsai, D. P. & Zheludev, N. I. Toroidal dipolar response in a metamaterial. *Science* **330**, 1510-1512 (2010).
45. Zhang, F. *et al.* Microwave Conference, 2008. EuMC 2008. 38th European 2008; Vol. 1, 801-804.
46. Shen, Y.; Ai, Q. Optical properties of drug metabolites in latent fingerprints. *Sci. Rep.* **6**, 20336 (2016).
47. Groeneveld, G., de Puit, M., Bleay, S., Bradshaw, R. & Francese, S. Detection and mapping of illicit drugs and their metabolites in fingerprints by MALDI MS and compatibility with forensic techniques. *Sci. Rep.* **5**, 11716 (2015).
48. Wei, T. T. *et al.* Metabonomic analysis of potential biomarkers and drug targets involved in diabetic nephropathy mice. *Sci. Rep.* **5**, 11998 (2015).
49. Dong, W. B., Wu, R. B., Yuan, X. H., Li, C. W. & Tarn, T.-J. The modelling of quantum control systems. *Sci. Bull.* **60**, 1493 (2015).
50. Shen, Y., Ko, H.-Y., Ai, Q., Peng, S.-M. & Jin, B.-Y. Molecular split-ring resonators based on metal string complexes. *J. Phys. Chem. C* **118**, 3766-3773 (2014).
51. Salem, L. *The molecular orbital theory of conjugated systems* (W. A. Benjamin, New York, 1966).
52. Tokuji, S. A. *et al.* Facile formation of a benzopyrane-fused [28] hexaphyrin that exhibits distinct Möbius aromaticity. *J. Am. Chem. Soc.* **131**, 7240-7241 (2009).
53. Hawke, L., Kalosakasa, G. & Simserides, C. Empirical LCAO parameters for pi molecular orbitals in planar organic molecules. *Mol. Phys.* **107**, 1755-1771 (2009).
54. Harrison, W. A. *Electronic structure and the properties of solids* 2nd edn (Dover, New York, 1989).
55. Harrison, W. A. *Elementary electronic structure* (World Scientific, New Jersey, 1999).
56. NIST Chemistry Webbook and references therein. Available at: <http://webbook.nist.gov/chemistry/>. (Accessed: 4th December 2015).

## Author contributions statement

Yao Shen designed the project, wrote the main manuscript text and did the calculations. Yu-Zhu Chen reviewed the manuscript.

## Additional information

Competing financial interests: The authors declare no competing financial interests.